THz generation at 1.55 µm excitation: six-fold increase in THz conversion efficiency by separated photoconductive and trapping regions

Roman J. B. Dietz,[1,*] Marina Gerhard,[1] Dennis Stanze,[1] Martin Koch,[2] Bernd Sartorius,[1] and Martin Schell[1]

[1]*Fraunhofer Instiute for Telecommunications, Heinrich-Hertz-Institute, Einsteinufer 37,10587 Berlin, Germany*
[2]*Department of Physics, Philipps-Universität Marburg, Renthof 5, 35032 Marburg, Germany*
[*]*Roman.Dietz@hhi.fraunhofer.de*

Abstract: We present first results on photoconductive THz emitters for 1.55µm excitation. The emitters are based on MBE grown $In_{0.53}Ga_{0.47}As/In_{0.52}Al_{0.48}As$ multilayer heterostructures (MLHS) with high carrier mobility. The high mobility is achieved by spatial separation of photoconductive and trapping regions. Photoconductive antennas made of these MLHS are evaluated as THz emitters in a THz time domain spectrometer (THz TDS). The high carrier mobility and effective absorption significantly increases the optical-to-THz conversion efficiency with THz bandwidth in excess of 3 THz.

OCIS codes: (260.5150) Photoconductivity; (300.6495) Spectroscopy, terahertz; (160.5140) Photoconductive materials; (040.5150) Photoconductivity.

References and links

1. P. Jepsen, D. G. Cooke, and M. Koch, "Terahertz spectroscopy and imaging – Modern techniques and applications," Laser Photon. Rev. **5**(1), 124–166 (2011), http://onlinelibrary.wiley.com/doi/10.1002/lpor.201000011/abstract.
2. M. B. Ketchen, D. Grischkowsky, T. C. Chen, C.-C. Chi, I. N. Duling, N. J. Halas, J.-M. Halbout, J. A. Kash, and G. P. Li, "Generation of sub-picosecond electrical pulses on coplanar transmission lines," Appl. Phys. Lett. **48**(12), 751–753 (1986), http://link.aip.org/link/doi/10.1063/1.96709.
3. P. R. Smith, D. H. Auston, and M. C. Nuss, "Subpicosecond photoconducting dipole antennas," IEEE J. Quantum Electron. **24**(2), 255–260 (1988), http://dx.doi.org/10.1109/3.121.
4. A. C. Warren, N. Katzenellenbogen, D. Grischkowsky, J. M. Woodall, M. R. Melloch, and N. Otsuka, "Subpicosecond, freely propagating electromagnetic pulse generation and detection using GaAs:As epilayers," Appl. Phys. Lett. **58**(14), 1512–1514 (1991), http://link.aip.org/link/doi/10.1063/1.105162.
5. H. M. Heiliger, M. Vosseburger, H. G. Roskos, H. Kurz, R. Hey, and K. Ploog, "Application of liftoff low-temperature-grown GaAs on transparent substrates for THz signal generation," Appl. Phys. Lett. **69**(19), 2903–2905 (1996), http://link.aip.org/link/doi/10.1063/1.117357.
6. S. Matsuura, M. Tani, and K. Sakai, "Generation of coherent terahertz radiation by photomixing in dipole photoconductive antennas," Appl. Phys. Lett. **70**(5), 559–561 (1997), http://link.aip.org/link/doi/10.1063/1.118337.
7. M. Tani, S. Matsuura, K. Sakai, and S. Nakashima, "Emission characteristics of photoconductive antennas based on low-temperature-grown GaAs and semi-insulating GaAs," Appl. Opt. **36**(30), 7853–7859 (1997), http://www.opticsinfobase.org/abstract.cfm?URI=ao-36-30-7853.
8. K. Ezdi, B. Heinen, C. Jördens, N. Vieweg, N. Krumbholz, R. Wilk, M. Mikulics, and M. Koch, "A hybrid time-domain model for pulsed terahertz dipole antennas," J. Eur. Opt. Soc. Rapid. Publ. **4**, 09001 (2009), http:/www.jeos.org/index.php/jeos_rp/article/view/09001.
9. N. Vieweg, M. Mikulics, M. Scheller, K. Ezdi, R. Wilk, H. W. Hübers, and M. Koch, "Impact of the contact metallization on the performance of photoconductive THz antennas," Opt. Express **16**(24), 19695–19705 (2008), http://www.opticsinfobase.org/abstract.cfm?URI=oe-16-24-19695.
10. K. A. McIntosh, K. B. Nichols, S. Verghese, and E. R. Brown, "Investigation of ultrashort photocarrier relaxation times in low-temperature-grown GaAs," Appl. Phys. Lett. **70**(3), 354–356 (1997), http://link.aip.org/link/doi/10.1063/1.118412.
11. M. Griebel, J. H. Smet, D. C. Driscoll, J. Kuhl, C. A. Diez, N. Freytag, C. Kadow, A. C. Gossard, and K. Von Klitzing, "Tunable subpicosecond optoelectronic transduction in superlattices of self-assembled ErAs nanoislands," Nat. Mater. **2**(2), 122–126 (2003), doi:10.1038/nmat819.

#155819 - $15.00 USD Received 3 Oct 2011; revised 7 Nov 2011; accepted 16 Nov 2011; published 5 Dec 2011

12. C. Kadow, A. W. Jackson, A. C. Gossard, S. Matsuura, and G. A. Blake, "Self-assembled ErAs islands in GaAs for optical-heterodyne THz generation," Appl. Phys. Lett. **76**(24), 3510–3512 (2000), http://link.aip.org/link/doi/10.1063/1.126690.
13. J. Sigmund, C. Sydlo, H. L. Hartnagel, N. Benker, H. Fuess, F. Rutz, T. Kleine-Ostmann, and M. Koch, "Structure investigation of low-temperature-grown GaAsSb, a material for photoconductive terahertz antennas," Appl. Phys. Lett. **87**(25), 252103 (2005), http://link.aip.org/link/doi/10.1063/1.2149977.
14. K. Bertulis, A. Krotkus, G. Aleksejenko, V. Pačebutas, R. Adomavičius, G. Molis, and S. Marcinkevičius, "GaBiAs: A material for optoelectronic terahertz devices," Appl. Phys. Lett. **88**(20), 201112 (2006), http://link.aip.org/link/doi/10.1063/1.2205180.
15. M. Suzuki and M. Tonouchi, "Fe-implanted InGaAs terahertz emitters for 1.56 μm wavelength excitation," Appl. Phys. Lett. **86**(5), 051104 (2005), http://link.aip.org/link/doi/10.1063/1.1861495.
16. M. Suzuki and M. Tonouchi, "Fe-implanted InGaAs photoconductive terahertz detectors triggered by 1.56 μm femtosecond optical pulses," Appl. Phys. Lett. **86**(16), 163504 (2005), http://link.aip.org/link/doi/10.1063/1.1901817.
17. A. Takazato, M. Kamakura, T. Matsui, J. Kitagawa, and Y. Kadoya, "Detection of terahertz waves using low-temperature-grown InGaAs with 1.56 μm pulse excitation," Appl. Phys. Lett. **90**(10), 101119 (2007), http://link.aip.org/link/doi/10.1063/1.2712503.
18. A. Takazato, M. Kamakura, T. Matsui, J. Kitagawa, and Y. Kadoya, "Terahertz wave emission and detection using photoconductive antennas made on low-temperature-grown InGaAs with 1.56 μm pulse excitation," Appl. Phys. Lett. **91**(1), 011102 (2007), http://link.aip.org/link/doi/10.1063/1.2754370.
19. R. Wilk, M. Mikulics, K. Biermann, H. Künzel, I. Z. Kozma, R. Holzwarth, B. Sartorius, M. Mei, and M. Koch, "THz Time-Domain Spectrometer Based on LT-InGaAs Photoconductive Antennas Exited by a 1.55 μm Fibre Laser, " in *Conference on Lasers and Electro-Optics/Quantum Electronics and Laser Science Conference and Photonic Applications Systems Technologies*, OSA Technical Digest Series (CD) (Optical Society of America, 2007), paper CThR2, http://ieeexplore.ieee.org/stamp/stamp.jsp?tp=&arnumber=4452856&isnumber=4452320.
20. B. Sartorius, H. Roehle, H. Künzel, J. Böttcher, M. Schlak, D. Stanze, H. Venghaus, and M. Schell, "All-fiber terahertz time-domain spectrometer operating at 1.5 microm telecom wavelengths," Opt. Express **16**(13), 9565–9570 (2008), http://www.opticsinfobase.org/abstract.cfm?URI=oe-16-13-9565.
21. A. Schwagmann, Z.-Y. Zhao, F. Ospald, H. Lu, D. C. Driscoll, M. P. Hanson, A. C. Gossard, and J. H. Smet, "Terahertz emission characteristics of ErAs:InGaAs-based photoconductive antennas excited at 1.55μm," Appl. Phys. Lett. **96**(14), 141108 (2010), http://link.aip.org/link/doi/10.1063/1.3374401.
22. C. D. Wood, O. Hatem, J. E. Cunningham, E. H. Linfield, A. G. Davies, P. J. Cannard, M. J. Robertson, and D. G. Moodie, "Terahertz emission from metal-organic chemical vapor deposition grown Fe:InGaAs using 830 nm to 1.55μm excitation," Appl. Phys. Lett. **96**(19), 194104 (2010), http://link.aip.org/link/doi/10.1063/1.3427191.
23. O. Hatem, J. Cunningham, E. H. Linfield, C. D. Wood, A. G. Davies, P. J. Cannard, M. J. Robertson, and D. G. Moodie, "Terahertz-frequency photoconductive detectors fabricated from metal-organic chemical vapor deposition-grown Fe-doped InGaAs," Appl. Phys. Lett. **98**(12), 121107 (2011), http://link.aip.org/link/doi/10.1063/1.3571289.
24. J. Oh, P. Bhattacharya, Y. Chen, O. Aina, and M. Mattingly, "The dependence of the electrical and optical properties of molecular beam epitaxial $In_{0.52}Al_{0.48}As$ on growth parameters: Interplay of surface kinetics and thermodynamics," J. Electron. Mater. **19**(5), 435–441 (1990), http://www.springerlink.com/content/010544084t85h872/.
25. H. Hoenow, H.-G. Bach, J. Böttcher, F. Gueissaz, H. Künzel, F. Scheffer, and C. Schramm, "Deep level Analysis of Si Doped MBE Grown AlInAs Layers, " Proc. 4th Int. Conf. InP and Rel. Mater., 136–139 (1992), http://ieeexplore.ieee.org/stamp/stamp.jsp?arnumber=00235658.
26. J. S. Weiner, D. S. Chemla, D. A. B. Miller, T. H. Wood, D. Sivco, and A. Y. Cho, "Room temperature excitons in 1.6μm band-gap GaInAs/AlInAs quantum wells," Appl. Phys. Lett. **46**(7), 619–621 (1985), http://link.aip.org/link/doi/10.1063/1.95504.
27. H. Künzel, J. Böttcher, R. Gibis, and G. Urmann, "Material properties of $Ga_{0.47}In_{0.53}As$ grown on InP by low-temperature molecular beam epitaxy," Appl. Phys. Lett. **61**(11), 1347–1349 (1992), http://link.aip.org/link/doi/10.1063/1.107587.
28. H. Roehle, R. J. B. Dietz, H. J. Hensel, J. Böttcher, H. Künzel, D. Stanze, M. Schell, and B. Sartorius, "Next generation 1.5 μm terahertz antennas: mesa-structuring of InGaAs/InAlAs photoconductive layers," Opt. Express **18**(3), 2296–2301 (2010), http://www.opticsinfobase.org/oe/abstract.cfm?URI=oe-18-3-2296.
29. P. U. Jepsen, R. H. Jacobsen, and S. R. Keiding, "Generation and detection of terahertz pulses from biased semiconductor antennas," J. Opt. Soc. Am. B **13**(11), 2424–2436 (1996), http://www.opticsinfobase.org/abstract.cfm?URI=josab-13-11-2424.

1. Introduction

Terahertz time domain spectroscopy (TDS) is by far the method of most importance within the rapidly developing and prosperous field of terahertz technology [1]. This method is based on the optical or optoelectronical generation and detection of short THz pulses by non-linear crystals or semiconductor based photoconductive antennas (PCA). In the latter case it is crucial to employ a material that exhibits very short carrier lifetimes in order to obtain broadband THz spectra.

#155819 - $15.00 USD Received 3 Oct 2011; revised 7 Nov 2011; accepted 16 Nov 2011; published 5 Dec 2011

The first generation of THz radiation from PCAs was achieved with radiation damaged silicon-on-sapphire [2,3]. Later experiments employed low temperature (LT) molecular beam epitaxy (MBE) grown GaAs, which rapidly became the state of the art material [4–6]. For all material systems the THz pulses were excited by titanium sapphire femtosecond lasers at wavelengths around 800 nm.

In the last 20 years there have been numerous approaches to increase the performance of photoconductive antennas, e.g. investigating antenna structure [7,8], metallization [9] and carrier lifetime [10] or by utilizing new material systems, such as GaAs:ErAs [11,12], LT GaAsSb [13] and GaAsBi [14]. The first attempt of PCAs based on InGaAs, for excitation with cost-effective fibre lasers at wavelengths around 1.55 µm, was made by Suzuki and Tonouchi [15,16] with ion-implanted InGaAs, followed by Takazato and Kadoya with LT-growth of InGaAs [17,18]. Subsequently, it was shown that LT MBE grown Beryllium doped InGaAs/InAlAs heterostructures are suitable for broadband THz emitters and detectors [19]. Followed by the introduction of a completely fibre coupled THz TDS system based on these antennas [20]. Since then other groups also demonstrated THz emission and detection in InGaAs based materials [21–23].

Despite these great efforts there is still vast potential for improvement of InGaAs based PCAs.As mentioned above, short carrier lifetimes are a key feature for broadband THz PCAs. These short carrier lifetimes are generally realized by inducing defect states into the respective semiconductor material. These defect states can be realized by strong doping [22,23], ion implantation [15,16], growth conditions, e.g. LT growth [17–19], or the growth of special recombination centers [21]. Additional important characteristics for efficient THz emitters are efficient absorption, a sufficiently high carrier mobility and high dark resistivity, i.e. low residual carrier concentrations.

However, it is difficult to fulfill all of the above requirements, since high defect material typically shows a strongly reduced carrier mobility due to elastic and inelastic (i.e. trapping) scattering of carriers at defect sites. Furthermore, in case of InGaAs the defects states are energetically situated relatively close to the conduction band. This shifts the Fermi level closer to the conduction band edge which results in low dark resistivity at room temperature.

The Fermi level can be lowered by counter doping with an acceptor-type dopant. However, counter doping further reduces carrier mobility. In addition, light absorption is also reduced in high defect materials.

In this work we present a new approach to circumvent some of these obstacles. The basic idea is to spatially separate the photoconductive region, i.e. where light absorption and carrier transport take place, from regions that exhibit high defect densities and that are transparent for 1.55 µm excitation, thus solely acting as trapping and recombination regions.

2.Principle and growth

A device meeting the above mentioned requirements can be realized by MBE growth of $In_{0.53}Ga_{0.47}As/In_{0.52}Al_{0.48}As$ multi-layer heterostructures (MLHS) (as depicted in Fig. 1(a)) when utilizing a special characteristic of MBE growth of InAlAs. Within a substrate temperature range between T_S = 300 - 500 °C the growth of InAlAs shows strong alloy clustering effects with InAs-like and AlAs-like regions featuring clusters sizes of several nanometers, with a maximum cluster density for $T_s \approx 400$ °C [24]. The activation energies of these cluster defects have been measured to be in the region of E_A = 0.6-0.7 eV [24,25] which results in the InAlAs to be semi-isolating. For the growth of a MLHS at this temperature and considering the conduction band offset between InAlAs (E_g = 1.47 eV at 300 K) and InGaAs (E_g = 0.74 eV at 300 K) of approximately ΔE_c = 0.44 eV [26], this results in defect states within the InAlAs layers that are energetically situated significantly below the conduction band of adjacent InGaAs layers, as depicted schematically in Fig. 1(b).

If the InAlAs layers are sufficiently thin, i.e. the the electron wave function of an optically excited electron in the conduction band of an InGaAs layer has a sufficiently large overlap with the cluster defect states in the adjacent InAlAs layer, these defects can act as effective traps for those electrons. In addition, the MBE growth of InGaAs at substrate temperatures

#155819 - $15.00 USD Received 3 Oct 2011; revised 7 Nov 2011; accepted 16 Nov 2011; published 5 Dec 2011

around 400 - 500 °C shows a minimum for the residual carrier concentration, with N_A-N_D < $3 \cdot 10^{-15}$ cm^{-3} and Hall mobility values for bulk material of $\mu_{H,InGaAs}$ = 10000 cm^2/Vs [27]. Hence, the growth of a InGaAs/InAlAs MLHS should lead to short carrier lifetimes while maintaining effective absorption, high dark resistivity and high carrier mobility in the photoconductive layer.

The InGaAs/InAlAs MLHS investigated in this work were grown by elemental source molecular beam epitaxy on semi insulating InP:Fe substrates at an approximate substrate temperature of 400 °C. First a 777 nm InAlAs buffer layer was grown followed by 100 periods of 12 nm InGaAs layers and 8 nm InAlAs layers.

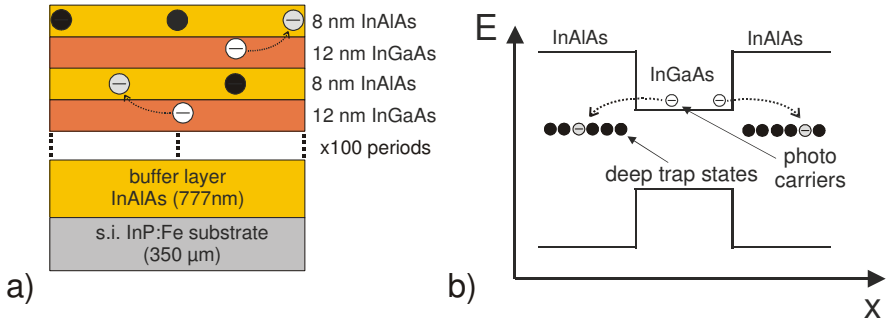

Fig. 1. (a) Schematic of InGaAs/InAlAs heterostructure, with 100 periods of a 12 nm InGaAs layer followed by a 8 nm InAlAs layer with cluster-induced defects acting as electron traps. 1(b) Schematic of the respective band-diagram in real space with deep cluster-induced defect states.

We measured Hall mobility values for the MLHS grown at T_S = 400 °C of $\mu_{H,400\text{-}MLHS}$ = 1500-3000 cm^2/Vs, with sheet carrier densities down to $N_s = 2.3 \cdot 10^8$ cm^{-2} and resistivity values of up to ρ = 5800 Ω·cm. The decrease in Hall mobility compared to the bulk InGaAs value is due to the fact that trapping of carriers into defect states in the InAlAs layers also contributes to the scattering time which is probed by hall mobility measurements. Nevertheless the mobility of the MLHS grown at 400°C is still almost one magnitude higher than that of LT-grown (T_S = 130°C) Be-doped MLHS with Hall mobility values of $\mu_{H,LT\text{-}MLHS}$ < 500 cm^2/Vs, with $N_s = 1.4 \cdot 10^{10}$ cm^{-2} and ρ = 240 Ω·cm.

3. THz TDS measurements

In order to evaluate the 400 °C grown material as a THz emitter, the samples were processed as mesa-type antennas as described in [28] with a stripline type antenna geometry and a stripline separation of 25 µm. A similarly structured conventional LT grown Be-doped InGaAs/InAlAs MLHS served as a reference emitter in all measurements. For detection we used a photoconductive receiver also based on LT-grown Be-doped InGaAs/InAlAs MLHS processed with a 10 µm gap dipole mesa-type antenna. The THz TDS setup consisted of a pre-compensated pulsed Er-doped fibre laser with a repetition rate of 100 MHz and pulses with approximately 80 fs FWHM pulse width. The laser was focused onto the emitter and detector with a spot size of approximately 10 µm. The THz beam path consisted of hyper-hemispherical silicon lenses attached to the backside of each antenna and two off-axis parabolic mirrors in between to focus the THz emission onto the detector. The overall THz path length was approximately 20 cm. A mechanical delay stage was used to introduce a delay between the optical pump and probe pulse, with a used time resolution of 50 fs. The emitters were fed with a bias modulated form 0 V to 5 V and a modulation frequency of 500 Hz. The lock-in time constant was 30 ms. Figure 2 shows the Fourier spectrum of the signal from the LT-reference antenna with the corresponding THz pulse trace in the inset. Figure 3 shows the FFT spectrum and THz pulse obtained from the new emitter material. The optical excitation was 10 mW at the emitter and 20 mW at the detector.

#155819 - $15.00 USD Received 3 Oct 2011; revised 7 Nov 2011; accepted 16 Nov 2011; published 5 Dec 2011

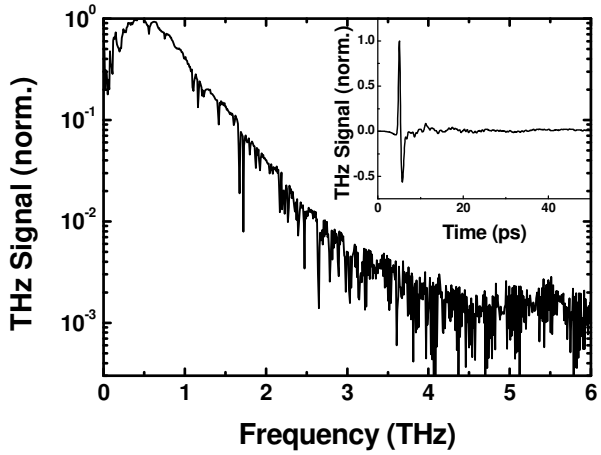

Fig. 2. THz pulse trace and corresponding FFT spectrum for a conventional LT-grown Be-doped MLHS THz emitter grown at T_s = 130 °C (this is serves as a reference).

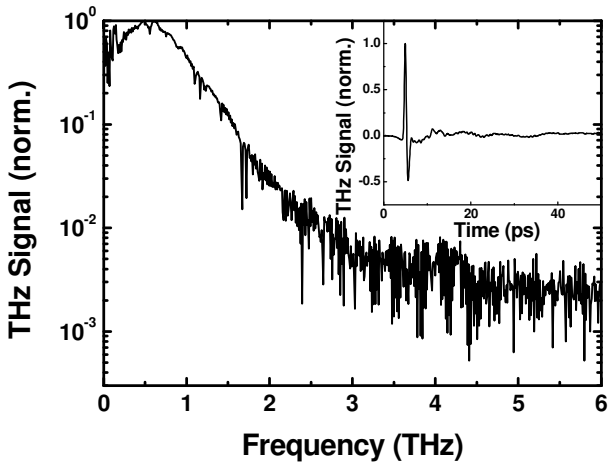

Fig. 3. THz pulse trace and corresponding FFT Spectrum for a MLHS grown at T_s = 400°C, with separated trapping and photoconductive regions.

As can be seen the spectral bandwidth of the new design is comparable to the one obtained with the LT grown reference, both extending well beyond 3 THz. The high bandwidth obtained with the new device suggests that the device exhibits relatively fast carrier trapping times, thus supporting the assumption of an effective trapping mechanism within the device. To further assess the carrier life time a dipol antenna, similar to that of the before used LT-grown detector, was deposited on the 400 °C grown material. This detector was then used in the TDS setup employing the LT-grown reference emitter as a source. The obtained FFT spectrum and pulse trace are depicted in Fig. 4. The detected THz spectrum extends beyond 3 THz, which further supports the assumption of short carrier life times in the 400 °C grown MLHS.

#155819 - $15.00 USD Received 3 Oct 2011; revised 7 Nov 2011; accepted 16 Nov 2011; published 5 Dec 2011

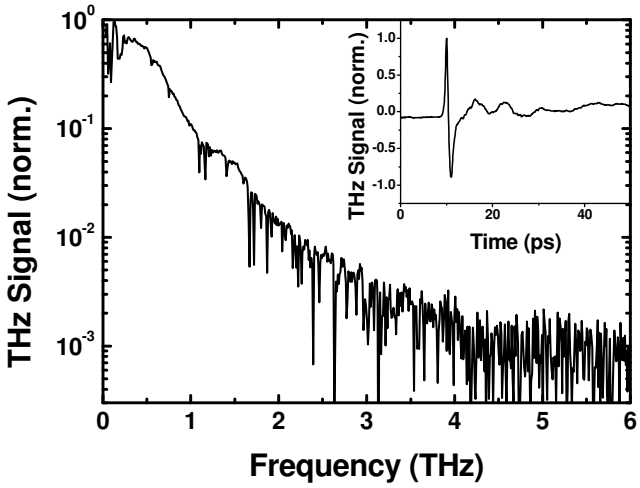

Fig. 4. THz pulse trace and corresponding FFT spectrum for the LT-grown Be-doped MLHS reference emitter grown at T_s = 130 °C and a T_s = 400° C grown receiver with a Dipol antenna.

4. Dependence on bias field and optical-to-THz conversion efficiency

To further evaluate the new material, we measured the peak-to-peak amplitude of the THz pulse obtained by TDS measurements in dependence of the applied bias field as well as in dependence on the optical power incident on the emitter antenna. Again an LT grown Be-doped MLHS antenna served as a reference. The THz amplitude over applied bias field is shown in Fig. 4. As can be seen the new MLHS grown at 400°C shows a much stronger THz emission than the LT reference. We attribute this to the improved carrier mobility in the new material. This can be understood within the framework of the classical Maxwell and Drude-model [29], where the emitted THz field is directly proportional to the derivative of the time varying photocurrent which is proportional to mobility. The measured DC photocurrents in the 400°C MLHS where strongly increased, e.g. for a bias field of 2kV/cm the DC photocurrents were I_p = 516 µA for the MLHS grown at 400°C and I_p = 9 µA for the LT grown material. This significant difference can't be explained by the higher mobility alone. We assume that the trapping time for the 400°C grown MLHS is slightly higher than for LT-grown MLHS. Additionally, the density of trap states in the 400°C is assumed to be smaller than for the LT-grown MLHS reference. This in turn results in a higher amount of long-lived carriers. This fact combined with the higher mobility lead to a strongly increased DC photocurrent. In Fig. 5 the THz amplitude is shown in dependence of the optical excitation power at the emitter for a constant bias field of 2 kV/cm. The new material shows a significantly higher light sensitivity compared to the LT reference, which we attribute to a shaper absorption band edge and the higher mobility in the 400 °C grown material compared to the LT-grown material.

#155819 - $15.00 USD Received 3 Oct 2011; revised 7 Nov 2011; accepted 16 Nov 2011; published 5 Dec 2011

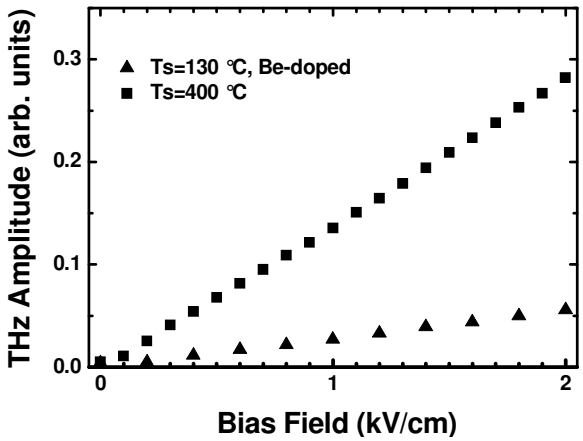

Fig. 5. Emitted THz-pulse amplitude detected by a PCA receiver in a THz TDS setup, as a function of applied bias field at the emitter for a MLHS grown at T_s = 400 °C (squares) and a MLHS grown at T_s = 130 °C, Be-doped (triangles). The applied optical power was 10 mW for both emitter and receiver.

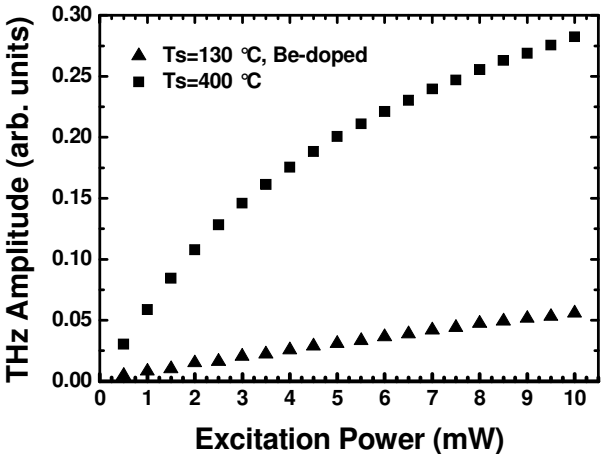

Fig. 6. Emitted THz-pulse amplitude detected by a PCA receiver in a THz TDS setup, as a function of optical excitation power at the emitter for a MLHS grown at T_s = 400 °C (squares) and a MLHS grown at T_s = 130 °C, Be-doped (triangles). The applied emitter bias field was 2 kV/cm.

5. Conclusion and outlook

We presented a new concept and the first realization of InGaAs based THz emitters that combine fast trapping times with high mobility and efficient absorption. The new emitters are capable of broadband THz emission while raising the optical-to-THz conversion efficiency by almost one order of magnitude. Future designs comprising optimized growth conditions and trapping layer thicknesses will potentially further improve the performance of these pulsed THz emitters.

Acknowledgments

We thank Deutsche Forschungsgemeinschaft for funding this work under grant KO 1520/5-1 and SA/784/4-1.

#155819 - $15.00 USD Received 3 Oct 2011; revised 7 Nov 2011; accepted 16 Nov 2011; published 5 Dec 2011